93Nb- and 27Al-NMR/NQR studies of the praseodymium based PrNb2Al20

Kubo, Tetsuro ; Kotegawa, Hisashi ; Tou, Hideki ; Higashinaka, Ryuji ; Nakama, Akihiro ; Aoki, Yuji ; Sato, Hideyuki

(Citation)
Journal of Physics: Conference Series,592:012093-012093

(Issue Date)
2015

(Resource Type)
journal article

(Version)
Version of Record

(URL)
https://hdl.handle.net/20.500.14094/90003374

^{93}Nb- and ^{27}Al-NMR/NQR studies of the praseodymium based $PrNb_2Al_{20}$

2015 J. Phys.: Conf. Ser. 592 012093

(http://iopscience.iop.org/1742-6596/592/1/012093)

Journal of Physics: Conference Series **592** (2015) 012093 doi:10.1088/1742-6596/592/1/012093

^{93}Nb- and ^{27}Al-NMR/NQR studies of the praseodymium based $PrNb_2Al_{20}$

Tetsuro Kubo[1,*], Hisashi Kotegawa[1], Hideki Tou[1,†], Ryuji Higashinaka[2], Akihiro Nakama[2], Yuji Aoki[2], and Hideyuki Sato[2]

[1]Department of Physics, Graduate School of Science, Kobe University, 1-1 Rokkodai, Kobe, Hyogo 657-8501, Japan

[2]Department of Physics, Graduate School of Science and Engineering, Tokyo Metropolitan University, 1-1 Minamiohsawa, Hachioji, Tokyo 192-0397, Japan

E-mail: *tkubo@stu.kobe-u.ac.jp †tou@crystal.kobe-u.ac.jp

Abstract. We report a study of ^{93}Nb- and ^{27}Al-nuclear magnetic resonance (NMR) and nuclear quadrupole resonance (NQR) in a praseodymium based compound $PrNb_2Al_{20}$. The observed NMR line at around 3 T and 30 K shows a superposition of typical powder patterns of one Nb signal and at least two Al signals. ^{93}Nb-NMR line could be reproduced by using the previously reported NQR frequency $\nu_Q \simeq 1.8$ MHz and asymmetry parameter $\eta \simeq 0$ [Kubo T *et al* 2014 *JPS Conf. Proc.* **3** 012031]. From ^{27}Al-NMR/NQR, NQR parameters are obtained to be $\nu_{Q,A} \simeq 1.53$ MHz, and $\eta_A \simeq 0.20$ for the site A, and $\nu_{Q,B} \simeq 2.28$ MHz, and $\eta_B \simeq 0.17$ for the site B. By comparing this result with the previous ^{27}Al-NMR study of PrT_2Al_{20} (T = Ti, V) [Tokunaga Y *et al* 2013 *Phys. Rev.* B **88** 085124], these two Al site are assigned to the two of three crystallographycally inequivalent Al sites.

1. Introduction

Cubic Pr compounds have attracted much attention for a long time because of their intriguing phenomena.[1, 2, 3] Recently, PrT_2X_{20} compounds (T = Ir, Ti, V, Nb, X = Zn, Al) show quadrupolar ordering, unconventional superconductivity, and non-Fermi liquid (NFL) behaviors at low temperatures.[4, 5, 6, 7, 8, 9] In these systems, Pr-4f electron can have a nonmagnetic crystalline electric field (CEF) Γ_3 doublet ground state which is magnetic dipolar inactive but higher order multipolar active. In general, Pr-4f electron is strongly localized because of its strong Hund coupling. However, in PrT_2X_{20}, each of Pr atoms is encapsulated in a cage consisted by 16 X atoms as shown in Fig.1. Thus, this large coordination number leads strong c-f hybridization. The coexistence of these characteristic features manifests novel phenomena. For example, $PrIr_2Zn_{20}$ shows antiferroquadrupolar (AFQ) ordering at $T_Q = 0.11$ K and superconductivity at $T_c = 0.05$ K.[4, 6] $PrTi_2Al_{20}$ shows ferroquadrupolar (FQ) ordering at $T_Q = 2.4$ K and superconductivity at $T_c = 0.2$ K.[7, 8] PrV_2Al_{20} shows AFQ ordering at $T_Q = 0.75$ K, superconductivity at $T_Q = 0.05$ K, and NFL behaviors such as resisitivity $\rho_{4f} \propto \sqrt{T}$, susceptibility $\chi_{4f} \propto -\sqrt{T}$, and specific heat divided by temperature $C_{4f}/T \propto T^{1.5}$.[7, 9] These behaviors are ascribed to the quadrupolar degree of freedom of the Γ_3 ground state. The relation between NFL behaviors and quadrupolar Kondo effect proposed by Cox[10] has been also discussed.

Recently, Higashinaka and co-workers successfully synthesized single crystal $PrNb_2Al_{20}$.[5] No phase transition was observed down to 0.6 K unlike other PrT_2X_{20}. Below 10 K, NFL behaviors such as $\rho_{4f} \propto T$ and $C_{4f}/T \propto -\ln T$ were observed. These behaviors may be attributed to the quadrupolar degree of freedom, although no clear CEF level scheme is determined.

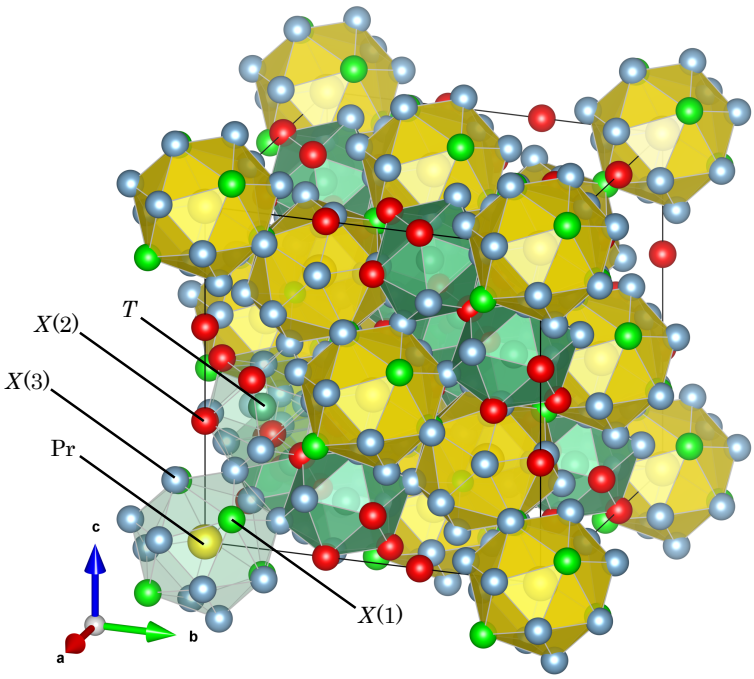

Figure 1. A schematic crystal structure of PrT_2X_{20}.

In $PrNb_2Al_{20}$, Al atoms occupy three crystallographically inequivalent sites: Al(1) is 16*c* site, Al(2) is 48*f* site, and Al(3) is 96*g* site. We previously reported ^{93}Nb nuclear magnetic resonance (NMR) and nuclear quadrupole resonance (NQR) studies and determined ^{93}Nb-NQR parameters as NQR frequency $\nu_Q \simeq 1.8$ MHz, and asymmetry parameter $\eta \simeq 0$.[11] However, ^{27}Al-NQR parameters could not obtained yet because of the multiple inequivalent Al sites.

In this paper, we report the results of ^{93}Nb- and ^{27}Al-NMR and NQR measurements on $PrNb_2Al_{20}$.

2. Experimental

Single crystal samples of $PrNb_2Al_{20}$ were prepared by Al-flux method. Details of sample preparation method are previously reported in [5]. In order to gain signal intensity, samples were crushed into powder to avoid skin effect due to eddy current. NMR measurements were performed using a 12 T superconducting magnet and a phase-coherent pulsed spectrometer at magnetic fields around $\mu_0 H$ = 3 T and 7 T. NQR measurements were performed using a glass dewar at 4.2 K. ^{93}Nb (nuclear spin $I = 9/2$, nuclear gyromagnetic ratio $^{93}\gamma_n/2\pi = 10.452$ MHz / T, and nuclear quadrupole moment $Q = -0.320 \times 10^{-28}$ m^{-2})- and ^{27}Al ($I = 5/2$, $^{27}\gamma_n/2\pi = 11.103$ MHz / T, and $Q = -0.1466 \times 10^{-28}$ m^{-2})-NMR/NQR spectra were obtained by tracing spin-echo intensity as a function of the resonance field and frequency.

3. Results and Discussion

Figure 2 exhibits a NMR line obtained at fixed frequency $f = 31.700$ MHz and $T = 30$ K. The line is considered to be a superposition of typical powder pattern lines. In order to reproduce the ^{93}Nb- and ^{27}Al-NMR lines, we calculated resonance field for powder samples by an exact-diagonalization method

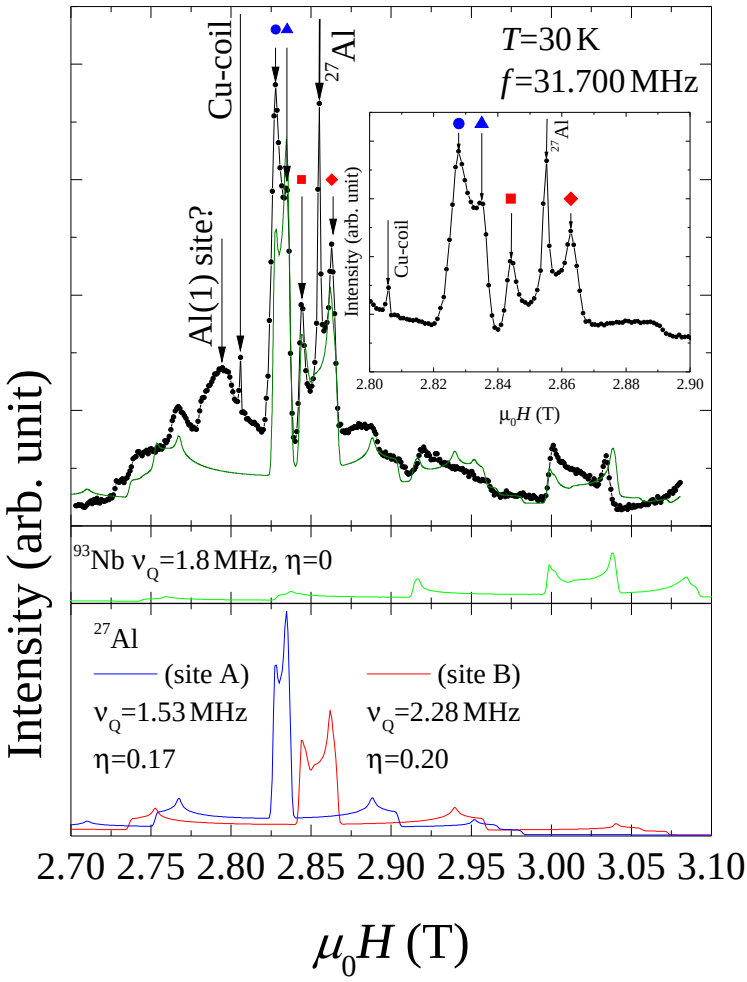

Figure 2. The NMR line obtained at around $\mu_0 H = 3\,\mathrm{T}$ and $T = 30\,\mathrm{K}$. A ^{63}Cu signal arises from the coil. A ^{27}Al signal may arise from the impurity. The inset exhibits the enlarged line profile around ^{27}Al central lines. A light green line shows the result of the simulation for ^{93}Nb. Red and blue lines indicates the result of the simulation for ^{27}Al. A dark green line is the sum of one ^{93}Nb line and two ^{27}Al lines. Detail of the simulation is explained in the text.

for a $(2I+1)\times(2I+1)$ nuclear spin hamiltonian matrix. The hamiltonian is expressed as

$$\begin{aligned}\mathcal{H} = -\gamma_{\mathrm{n}}\hbar I_z H_0 + \frac{1}{6}h\nu_{\mathrm{Q}}\Bigg\{&\frac{1}{2}\left[\left(3\cos^2\theta - 1\right) + \eta\sin^2\theta\cos 2\phi\right]\left(3I_z^2 - I^2\right)\\ &+ \frac{1}{4}\sin 2\theta\left(3 - \eta\cos 2\phi\right)\left[I_z\left(I_+ + I_-\right) + \left(I_+ + I_-\right)I_z\right] + \frac{1}{4}\left[3\sin^2\theta + \eta\left(1+\cos^2\theta\right)\cos 2\phi\right]\left(I_+^2 + I_-^2\right)\\ &+ \frac{i}{2}\eta\sin\theta\sin 2\phi\left[I_z\left(I_+ - I_-\right) + \left(I_+ - I_-\right)I_z\right] - \frac{i}{2}\eta\cos\theta\sin 2\phi\left(I_+^2 - I_-^2\right)\Bigg\}. \qquad (1)\end{aligned}$$

The first term represents to the Zeeman interaction. The second term corresponds to the nuclear quadrupole interaction. Here, h is Planck constant and $\hbar \equiv h/2\pi$. $\nu_{\mathrm{Q}} \equiv 3e^2qQ/2hI(2I-1)$ denotes the NQR frequency where $eq \equiv V_{ZZ}$ is the maximum principal value of the electric field gradient (EFG) tensor at each site. $\eta \equiv (V_{XX} - V_{YY})/V_{ZZ}$ exhibits the asymmetry parameter. V_{XX} and V_{YY} are the principal values of the EFG tensor satisfying $|V_{ZZ}| \geq |V_{YY}| \geq |V_{XX}|$ hence $0 \leq \eta \leq 1$. Here, θ and ϕ are polar and azimuth angle, respectively between the Zeeman coordinate and the EFG coordinate. For

simplicity, we neglected the anisotropy of Knight shift.

A light green solid line in Fig. 2 is the result of the simulation using $\nu_Q = 1.8$ MHz and $\eta = 0$. The agreement between experimental and calculated ones is good thus the validity of previously obtained NQR parameters is confirmed.

As shown in Fig. 2, several sharp peaks were observed. The central line of the NMR powder pattern spectrum (corresponding to $(-1/2 \leftrightarrow +1/2)$ transition) can be split by the second order perturbation of the nuclear quadrupole interaction. Here, we assumed that peaks around 2.825 and 2.835 T (● and ▲) originate from one Al site (site A) and peaks around 2.845 and 2.865 T (■ and ♦) originate from another Al site (site B). Theoretically, the width of splitting of the central line $\Delta\nu$ by the second order perturbation is expressed as

$$\Delta\nu = \frac{25\nu_Q^2[I(I+1) - 3/4]}{144\nu_0} \tag{2}$$

where $\nu_0 = \gamma H$ is the Zeeman frequency in the absence of nuclear quadrupole interaction.[12] By using eq. (2) , $I = 5/2$, and $\nu_0 = 31.700$ MHz, we extracted ν_Q as $\nu_{Q,A} \simeq 1.5$ MHz for the site A and $\nu_{Q,B} \simeq 2.3$ MHz for the site B.

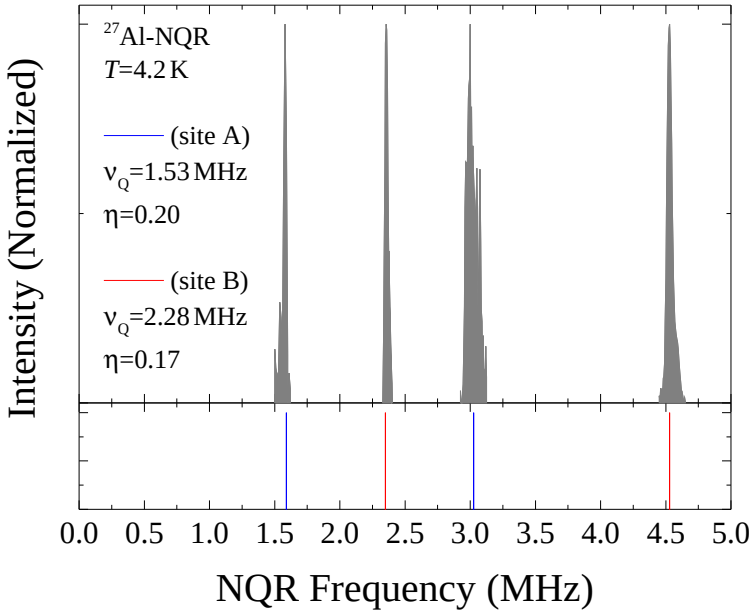

Figure 3. ^{27}Al-NQR lines obtained at $T = 4.2$ K. Intensities are normalized. Red and blue solid lines are the simulated transition lines explained in the text.

Next, we calculated resonance frequencies for NQR by using these ν_Q and eq. (1). Figure 3 shows ^{27}Al-NQR lines obtained at 4.2 K and the results of the simulation. ν_Q and η are estimated by the trial and error method, and are obtained to be $\nu_{Q,A} \simeq 1.53$ MHz, $\eta_A \simeq 0.20$ and $\nu_{Q,B} \simeq 2.28$ MHz, $\eta_B \simeq 0.17$ for sites A and B, respectively. The agreement between experimental and calculated results is satisfactory good.

The red and blue solid lines in Fig. 2 are the results of the simulation using these NQR parameters. The dark green line shows the sum of these three (one Nb and two Al) simulations. The simulation well reproduces the experimental line. However, lines around 2.80 T could not be reproduced. We speculate that this signal originates from Al(1) site because of its small fraction against lines from sites A and B.

Tokunaga and co-workers performed ^{27}Al-NMR experiments for single crystal PrT_2Al_{20} (T = Ti, V), and determined ^{27}Al-NQR parameters.[13] In Tab. 1, the ^{27}Al-NQR parameters for PrT_2Al_{20} (T = Nb, Ti, and V) are summarized. ν_Q and η of $PrNb_2Al_{20}$ are larger than the ones of $PrTi_2Al_{20}$ and PrV_2Al_{20}.

However, parameters of site B are close to the ones of Al(2) site. Thus, we speculate that site B corresponds to Al(2) site and site A corresponds to Al(3) site. To assign these ^{27}Al-NMR/NQR lines without ambiguity, the measurement of the temperature dependence of Knight shifts of these Al sites is essential and is now in progress.

Table 1. Comparison of ^{27}Al-NQR parameters of PrT_2Al_{20} (T = Nb, Ti, and V). ν_Q and η for T = Nb are obtained in the present study, and for T = Ti, V are taken from [13].

$PrNb_2Al_{20}$			$PrTi_2Al_{20}$			PrV_2Al_{20}		
Site	ν_Q (MHz)	η	Site	ν_Q (MHz)	η	Site	ν_Q (MHz)	η
A	~ 1.53	~ 0.20	Al(2)	2.03	0.145	Al(2)	1.90	0.145
B	~ 2.28	~ 0.17	Al(3)	0.92	0.39	Al(3)	0.84	0.30

4. Summary

We observed ^{93}Nb- and ^{27}Al-NMR/NQR signals of single crystal $PrNb_2Al_{20}$. From the spectral simulation, ^{93}Nb lines were well reproduced by using NQR parameters we previously reported. We deconvoluted the ^{27}Al-NMR/NQR lines and obtained ^{27}Al-NQR parameters to be $\nu_{Q,A} \simeq 1.53$ MHz and $\eta \simeq 0.20$ for site A and $\nu_{Q,B} \simeq 2.28$ MHz and $\eta \simeq 0.17$ for site B. By using these ^{93}Nb- and ^{27}Al-NQR parameters, the entire NMR line is well reproduced. In comparison with the result of $PrTi_2Al_{20}$ and PrV_2Al_{20}, site A and B correspond to Al(3) site and Al(2) site, respectively. These results allow us to investigate the microscopic electronic state and NFL behaviors of $PrNb_2Al_{20}$.

5. Acknowledgement

We gratefully thank Prof. H. Harima and Dr. S. Kitagawa for valuable discussions and helpful advice. This work has been supported by Grants-in-Aid for Scientific Research on Innovative Areas “Heavy Electrons” (Nos. 20102005 and 20102004) from MEXT of Japan. This work has also been supported by KAKENHI (24340085 and 26400359) of MEXT of Japan.

References

[1] Morin P, Schmitt D and du Tremolet de Lacheisserie E 1982 *J. Magn. Magn. Mater.* **30** 257
[2] Yatskar A, Beyermann W P, Movshovich R and Canfield P C 1996 *Phys. Rev. Lett.* **77** 3637
[3] Bauer E D, Frederick N A, Ho P-C, Zapf V S and Maple M B 2002 *Phys. Rev.* B **65** 100506
[4] Onimaru T, Matsumoto K T, Inoue Y F, Umeo K, Saiga Y, Matsushita Y, Tamura R, Nishimoto K, Ishii I, Suzuki T and Takabatake T 2010 *J. Phys. Soc. Jpn.* **79** 033704
[5] Higashinaka R, Nakama A, Ando M, Watanabe M, Aoki Y and Sato H 2011 *J. Phys. Soc. Jpn.* **80** SA048
[6] Onimaru T, Matsumoto K T, Inoue Y F, Umeo K, Sakakibara T, Karaki Y, Kubota M and Takabatake T 2011 *Phys. Rev. Lett.* **106** 177001
[7] Sakai A and Nakatsuji S 2011 *J. Phys. Soc. Jpn.* **80** 063701
[8] Sakai A, Kuga K and Nakatsuji S 2012 *J. Phys. Soc. Jpn.* **81** 083702
[9] Tsujimoto M, Matsumoto Y, Tomita T, Sakai A and Nakatsuji S 2014 *Phys. Rev. Lett.* **113** 267001
[10] Cox D L 1987 *Phys. Rev. Lett.* **59** 1240
[11] Kubo T, Kotegawa H, Tou H, Higashinaka R, Nakama A, Aoki Y and Sato H 2014 *JPS Conf. Proc.* **3** 012031
[12] Jones W H, Graham T P and Barnes R G 1963 *Phys. Rev.* **132** 1898
[13] Tokunaga Y, Sakai H, Kambe S, Sakai A, Nakatsuji S and Harima H 2013 *Phys. Rev.* B **88** 085124